This journal is © The Royal Society of Chemistry 2014

# Supramolecular Design of Low-dimensional Carbon Nano-hybrids encoding a Polyoxometalate-bis-Pyrene Tweezer

**Gloria Modugno,[a] Zois Syrgiannis,[b] Aurelio Bonasera,[b] Mauro Carraro,[a] Gabriele Giancane,[c] Ludovico Valli,*[,c] Marcella Bonchio,*[,a] and Maurizio Prato*[,b]**

[a] CNR-ITM and Department of Chemical Sciences, University of Padova, via F. Marzolo 1, 35131 Padova, Italy.
[b] Center of Excellence for Nanostructured Materials (CENMAT) and INSTM, unit of Trieste, Department of Chemical and Pharmaceutical Sciences, University of Trieste, Piazzale Europa 1, 34127 Trieste, Italy.
[c] Department of Biological and Environmental Sciences and Technologies, DISTEBA University of Salento Via per Arnesano, I-73100 Lecce, Italy.

## Materials.

HiPco SWNTs (Unidym™ HiPco® Single-Wall Carbon Nanotubes, batch P2771) have been purchased from Unidym™ and used without any further purification.

$C_{60}$ (BuckyUSA™ BU-602, Lot 06080101) has been purchased from BuckyUSA™ and used without any further purification.

$C_{70}$ (BuckyUSA™ BU-703, Lot gg01121) has been purchased from BuckyUSA™ and used without any further purification.

$(n\mathrm{Bu}_4\mathrm{N})_4[(\mathrm{NH}_2(\mathrm{CH}_2)_3\mathrm{Si})_2\mathrm{O}(\gamma\text{-}\mathrm{SiW}_{10}\mathrm{O}_{36})]$[i] and its precursor $\mathrm{K}_8[\gamma\text{-}\mathrm{SiW}_{10}\mathrm{O}_{36}]$[ii] were prepared following literature procedures.

Chemicals and solvents for synthesis and for carbon nanomaterials solubilisation have been purchased from Sigma-Aldrich and used as received.

## Equipment.

$^1$H NMR spectra have been recorded with Bruker AV300 instruments operating at 300.13 MHz; for protonic spectra, the following symbolism has been used: s: singlet; d: doublet; t: triplet; q: quartet; m: multiplet. $^{13}$C NMR spectra have been recorded with Bruker AV300 operating at 75.4 MHz; $\mathrm{Si(CH_3)_4}$ was used as reference. $^{183}$W NMR and $^{29}$Si NMR spectra have been recorded with a Bruker Avance DRX 400 instrument operating at 16.67 MHz and 79.50 MHz, respectively, using 2M $\mathrm{Na_2WO_4}$ in $\mathrm{D_2O}$ and $\mathrm{Si(CH_3)_4}$ in $\mathrm{CDCl_3}$ as external references.

FT-IR (KBr) spectra have been collected on a Thermo Quest Nicolet 5700 instrument. For FT-IR spectra the following symbolism has been used: w: weak signal; s: strong signal; b: broad signal.

ESI-MS spectra have been obtained with an Agilent LC/MSD Trap SL spectrometer, using a capillary potential of 1500V.

UV-Vis-NIR experiments have been performed at room temperature on a Varian Cary 5000 UV-Vis-NIR double beam spectrophotometer; 10 mm path length Hellma Analytics 100 QS quartz cuvettes have been used. Fluorescence UV-Vis spectra have been recorded on a Varian Cary Eclipse Fluorescence Spectrophotometer; 10 mm path length Hellma Analytics 117.100F QS quartz cuvettes have been used.

Zeta-potential was obtained by using a Malvern Zetasizer Nano ZS90 instrument, in polymethyl methacrylate (PMMA) cuvettes containing 1 ml of the solution under investigation.

Raman spectra were acquired with a Renishaw instrument, model Invia reflex equipped with 532, 633, and 785 nm lasers.

Thermogravimetric analyses have been performed on a TGA Q500 (TA Instruments) and recorded under $N_2$, upon equilibration at 100 °C, followed by a ramp of 10 °C/min up to 1000 °C. An appropriate quantity of material for performing TGA analysis has been collected only for **1**@HiPco.

Transmission electron microscopy (TEM) experiments have been performed using a Philips EM 208, accelerating voltage of 100 kV. Samples were prepared by sonication for 10 min and dropwise addition (8 µL) of the sample onto a carbon coated 200 mesh Ni grid (EM Sciences, Gibbstown, NJ) followed by solvent evaporation under vacuum.

For the AFM analysis, 100µl of each sample with a concentration of 2 µg/ml were spin coated (4000 rpm, 6 min) over Si wafer, gently rinsed with water and acetone, and blown with dry nitrogen, finally the samples were dry under vacuum in order to remove the excess of solvents. The samples have been characterized using a Nanoscope V (Digital Instruments Metrology Group, model MMAFMLN) in tapping mode in air at room temperature, using standard µmash® SPM probe (NSC15/AIBS) with tip height 20-25µm, cone angle <40° (Resonant frequency 325kHz, force constant of ~46N/m). Image analysis was performed with WsXM software (Nanotec Electronica S. L.).[iii]

## Methods.

### Synthesis of $(nBu_4N)_4[\{C_{16}H_9SO_2NH(CH_2)_3Si\}_2O(\gamma\text{-}SiW_{10}O_{36})]$ (1)

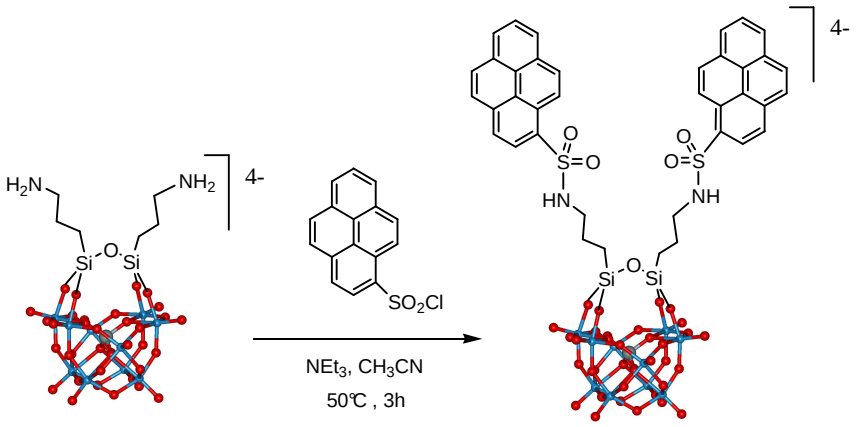


$(nBu_4N)_4[(NH_2(CH_2)_3Si)_2O\ (\gamma\text{-}SiW_{10}O_{36})]$ $(nBu_4N)_4[\{C_{16}H_9SO_2NH(CH_2)_3Si)_2O\ (\gamma\text{-}SiW_{10}O_{36})]$

*Scheme S1*

In a round bottomed flask, $(n\mathrm{Bu}_4\mathrm{N})_4[(\mathrm{NH}_2(\mathrm{CH}_2)_3\mathrm{Si})_2\mathrm{O}(\gamma\text{-}\mathrm{SiW}_{10}\mathrm{O}_{36})]$[iii] (450 mg, 0.14 mmol) was suspended in $CH_3CN$ (3 mL). After stirring for 5 min, triethylamine (49 µl, 0.35 mmol) was slowly added under vigorous stirring. 1-Pyrensulfonyl chloride (105 mg, 0.35 mmol) was dissolved in $CH_3CN$ (6 ml) and added dropwise in solution whilst stirring. The mixture was heated at 50°C for 3 h and then centrifuged to remove insoluble reagents and byproducts. The volume of the solution was reduced to 1 mL, upon evaporation under vacuum, than diethyl ether was added to precipitate the product. The solid was finally washed with water (2x5 mL), diethyl ether (2x5 mL), and a small amount of $CH_2Cl_2$ (2x5 mL) on a fritted funnel, and dried several hours under vacuum. 410 mg (0.1 mmol) of product were obtained (71% yield).

Elemental analysis: Calcd. for $C_{102}H_{176}N_6O_{41}S_2Si_3W_{10}$ C 29.67 H 4.30; N 2.04; S 1.55; Found: C 28.87; H 4.07; N 1.94; S 1.03. FT-IR (KBr): ν= 2961 (m), 2923 (m), 2873 (m), 1483 (m, b), 1385 (m), 1318 (w, b), 1159 (w), 1143 (w), 1132 (w), 1100 (m, b), 964 (m), 949 (m), 902 (s), 885 (s), 839 (s), 819 (s), 742 (s, b), 650 (w) $cm^{-1}$. $^1$H NMR (300 MHz, $CD_3CN$, 301 K) δ = 0.57 (4H, m, $NCH_2CH_2C\mathit{H}_2Si$), 0.94 (48H, t, $N(CH_2CH_2CH_2C\mathit{H}_3)_4$), 1.27 (4H, m, $NCH_2C\mathit{H}_2CH_2Si$), 1.34 (32H, m, $N(CH_2CH_2C\mathit{H}_2\mathit{C}H_3)_4$), 1.59 (32H, m, $N(CH_2C\mathit{H}_2CH_2\mathit{C}H_3)_4$), 3.09 (32 H, m, $N(C\mathit{H}_2CH_2CH_2\mathit{C}H_3)_4$), 3.54 (4H, m, $N\mathit{C}H_2CH_2CH_2Si$), 6.14 (2H, t, $^3J$ = 5.6 Hz, $\mathit{NH}CH_2CH_2CH_2Si$), 8.86 - 8.02 (18 H, m, Ar-H), ppm. $^{13}C\{^1H\}$NMR (75.47 MHz, $CD_3CN$, 301 K): δ = 12.35 (2C, $Si\mathit{C}H_2CH_2CH_2N$), 13.86 (16C, $N(CH_2CH_2CH_2\mathit{C}H_3)_4$), 20.29 (16C, $N(CH_2CH_2\mathit{C}H_2CH_3)_4$), 22.99 (2C, $SiCH_2\mathit{C}H_2CH_2N$), 24.32 (16C, $N(CH_2\mathit{C}H_2CH_2CH_3)_4$), 46.50 (2C, $SiCH_2CH_2\mathit{C}H_2N$), 59.24 (16C, $N(\mathit{C}H_2CH_2CH_2CH_3)_4$), 135.25-124.42 (32 C, Ar-*C*) ppm. $^{29}$Si NMR (79.5 MHz, $CD_3CN$/*d*-DMSO, 25°C): δ = -62.61 (2 Si), -88.34 (1 Si) ppm. $^{183}$W NMR (16.7 MHz, $CD_3CN$, 25°C): - 107.51 (4 W), -136.03 (2W), -141.52 (4 W) ppm. ESI-MS (–, $CH_3CN$): *m*/*z* = 789.5, 1053.1 expected for $[C_{38}H_{32}N_2O_{41}S_2Si_3W_{10}]^{4-}$ = 789.9; $[C_{38}H_{33}N_2O_{41}S_2Si_3W_{10}]^{3-}$ = 1053.5. ζ-potential (1 mg in 1.5 mL of $CH_3OH$:DMF=1:1) = -38.2 mV.

**Spectroscopic analyses of mixtures containing fullerenes and 1.**

A precise quantity of **1** (3 mg) was dispersed in 10 ml DMF and the solution was diluted six times (solution A). At the same time, a precise amount of fullerene (7.2 mg for $C_{60}$, 8.4 mg for $C_{70}$) was dissolved in 2 ml *o*-DCB and the solution was diluted six times (solution B). Dilutions have been performed in order to maintain a reasonable value of absorbance during the titrations. Absorption and emission titrations were performed upon stepwise addition of 4 µl of solution B ($5x10^{-3}$ M) into 2.7 mL of solution A (10 µM).

Concerning fluorescence experiments, excitation wavelength was generally set at 338 nm. For Stern-Volmer calculations, however, excitation wavelength was set at 350 nm, in order to minimize the absorption by fullerenes. Measurements were also corrected for the inner filter effect. At the emission position corresponding to half cell length (1/2 L), the absorption (optical density, OD) of the excitation light by the fullerenes at concentration C can be calculated by the following equations:

$$OD = Log\frac{I_0}{I} = \frac{1}{2}\varepsilon_{350}CL$$

$$F = F_1\frac{I_0}{I}$$

where $I_0/I$ is the ratio between the intensities of incident and transmitted excitation light, $\varepsilon_{350}$ is the molar absorption coefficient constant of the fullerenes, $F_1$ is the original fluorescence intensity measured from the spectra and $F$ is the corrected fluorescence intensity after deduction of the inner filter effect.

**Job plot experiments**

For the Job plot experiments, stock solutions of **1** (10.0 µM) in DMF (solution A) and fullerenes ($C_{60}$ or $C_{70}$) ($10^{-3}$ M) in *o*-DCB (solution B) were prepared. 11 solutions were prepared upon dilution, in DMF, of different quantities of A and B (solution 1: 20 µl A and 0 µl B; solution 2: 18 µl A and 2 µl B; solution 3: 16 µl A and 4 µl B; solution 4: 14 µl A and 6 µl B; solution 5: 12 µl A and 8 µl B; solution 6: 10 µl A and 10 µl B; solution 7: 8 µl A and 12 µl B; solution 8: 6 µlA and 14 µl B; solution 9: 4 µl A and 16 µl B; solution 10: 2 µl A and 18 µl B; solution 11: 0 µl A and 2 µl B). The total volume was fixed at 2.0 mL. The fluorescence intensity at 397 nm was then recorded ($\lambda_{ex}$ = 338 nm).

**Procedure followed for carbon nanotubes dispersion in the presence of 1.**

A precise quantity of **1** (3 mg) was dissolved in 3 ml DMF/MeOH 1:1 solution; after stirring the solution for 5 minutes, a precise quantity of **CNT**s (3 mg) was added. The mixture was treated with sonic bath irradiation for 30 minutes, and then stirred for further 30 minutes. The mixture was centrifuged for 1h at 3000 rpm, and the supernatant solution was collected. UV-Vis-NIR absorption and emission experiments were performed directly on the supernatant solutions without any dilution. Concerning fluorescence experiments, excitation wavelength was set at 335 nm. Recorded zeta-potential value was -12.9 mV.

# Spectra

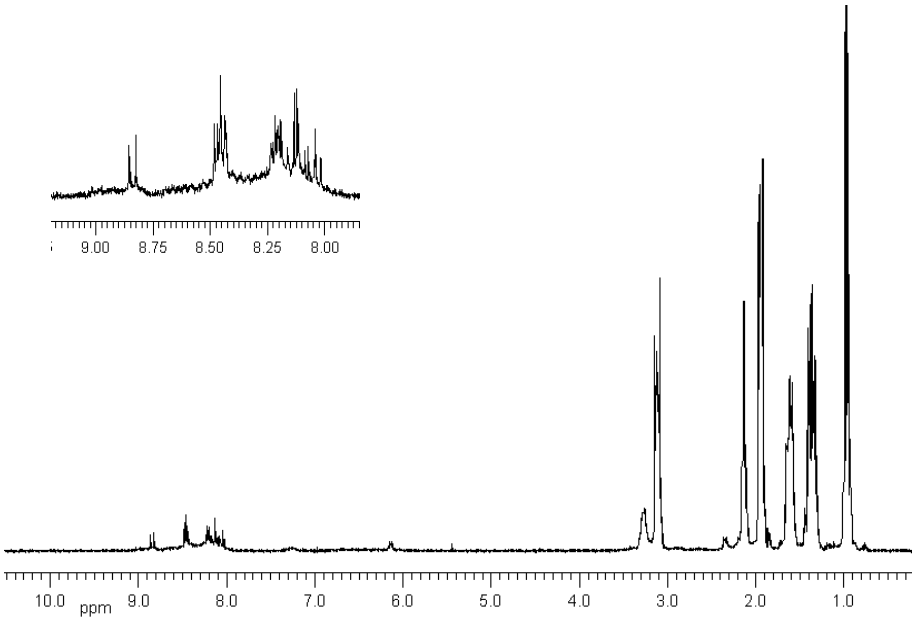


**Figure S1**: $^{1}$H-NMR spectrum of **1** in $CD_3CN$.

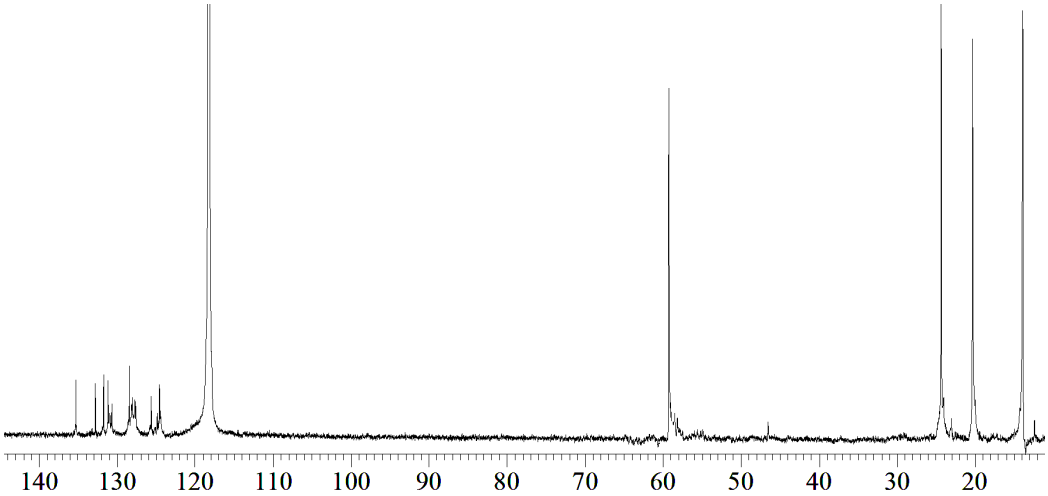


**Figure S2**: $^{13}$C-NMR spectrum of **1** in $CD_3CN$.

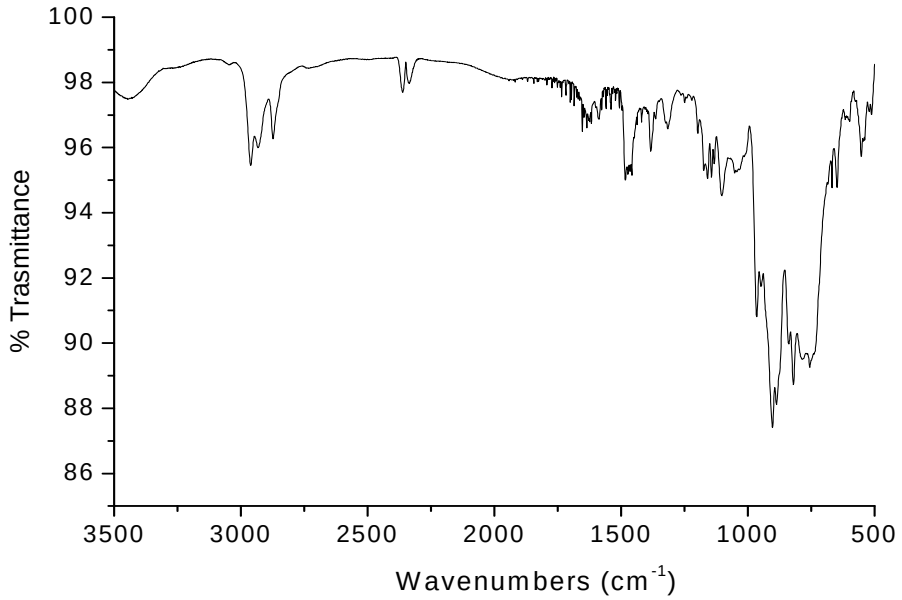


**Figure S3:** FT-IR (KBr) of **1.**

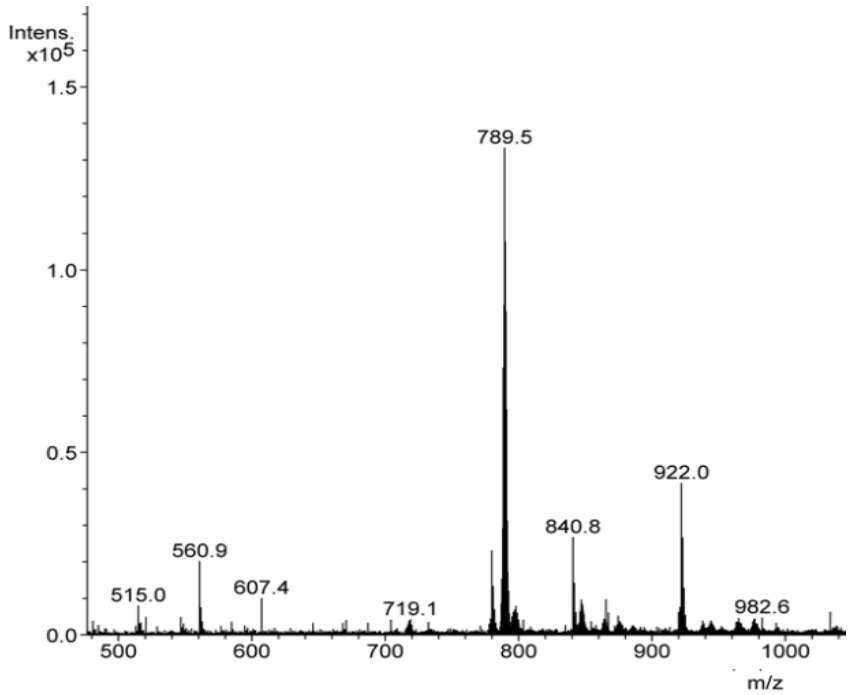


**Figure S4**: ESI-MS [(-), $CH_3CN$] of **1**.

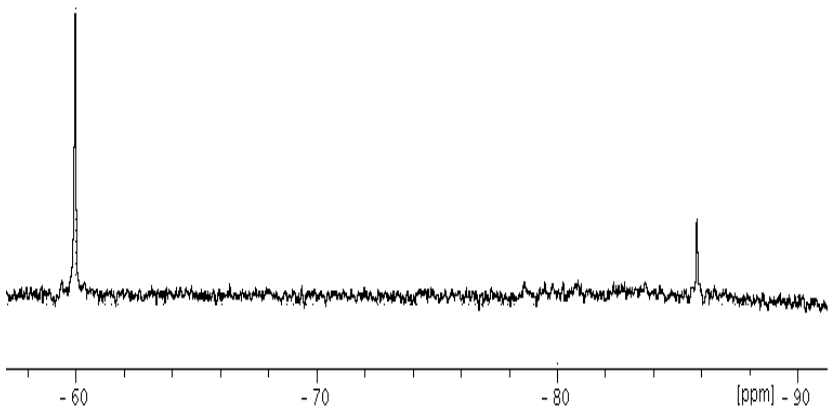


**Figure S5**: $^{29}$Si NMR spectrum of **1** in $CD_3CN$.

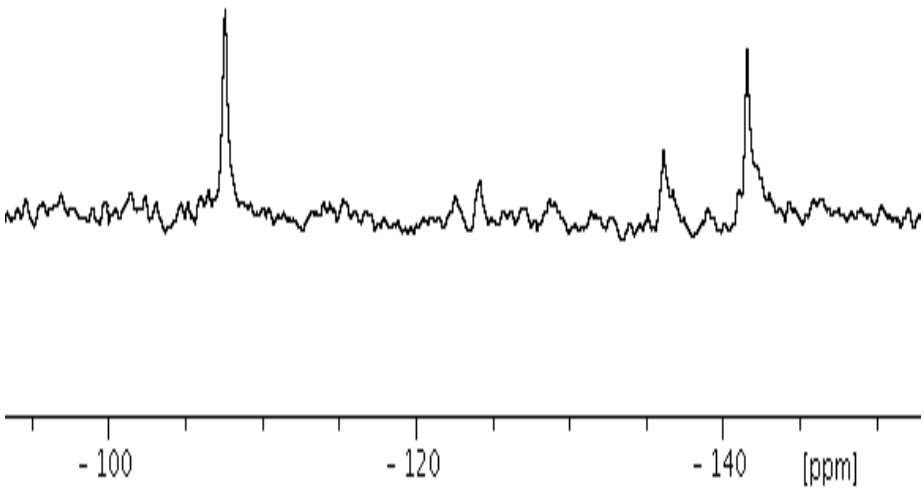


**Figure S6**: $^{183}$W NMR spectrum of **1** in $CD_3CN$.

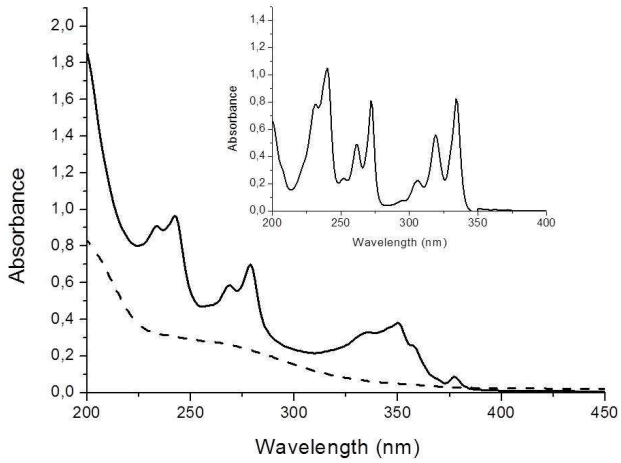


**Figure S7.** UV-Vis spectra of **1** (10 μM, solid line) and $(n\mathrm{Bu}_4\mathrm{N})_4[(\mathrm{NH}_2(\mathrm{CH}_2)_3\mathrm{Si})_2\mathrm{O}(\gamma\text{-}\mathrm{SiW}_{10}\mathrm{O}_{36})]$ (10 μM, dashed line) in $CH_3CN$; Inset: UV-vis spectrum of pyrene (20 μM) in $CH_3CN$.

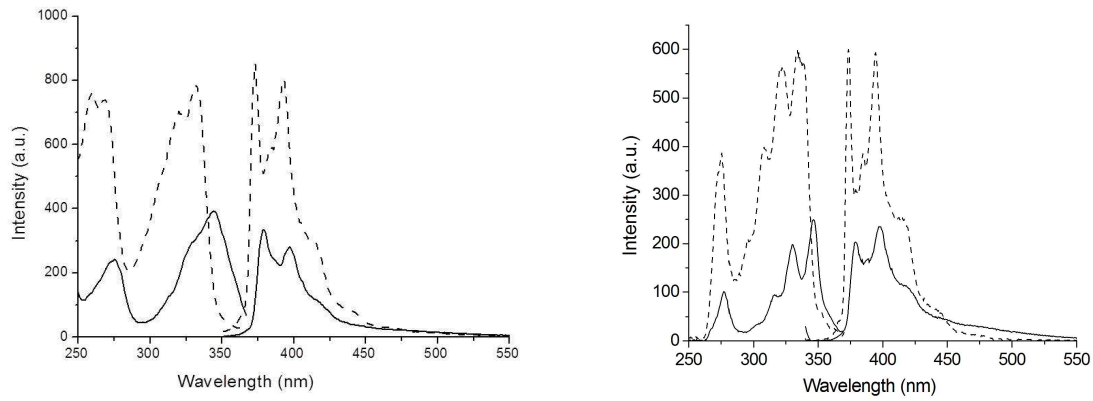


**Figure S8.** Fluorescence spectra of **1** [10 μM, solid lines: excitation ($\lambda_{em}$ = 380 nm) and emission ($\lambda_{exc}$ = 338 nm)] and pyrene [20 μM, dashed lines: excitation ($\lambda_{em}$ = 389 nm) and emission ($\lambda_{exc}$ = 338 nm)], in $CH_3CN$ (left), in DMF (right).

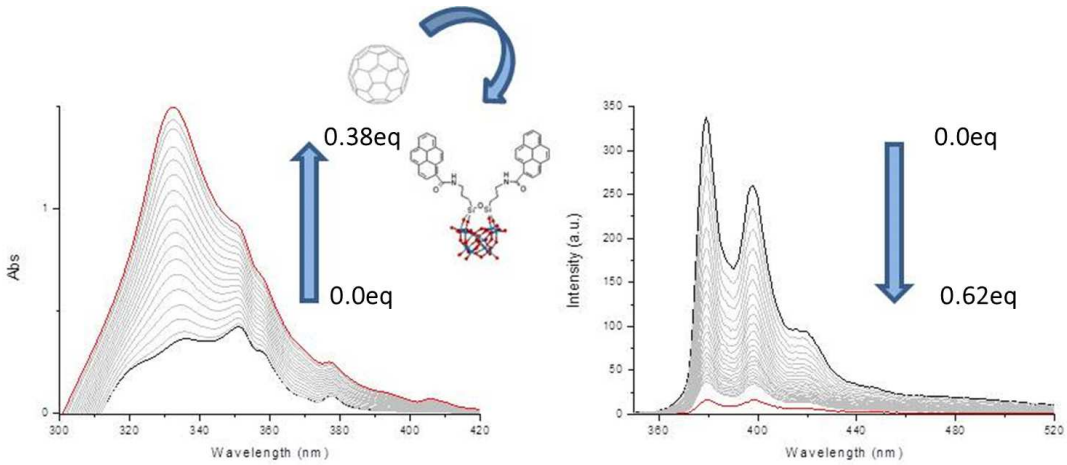


**Figure S9**. UV-vis (left) and fluorescence (right, $\lambda_{ex}$ = 338 nm) spectra obtained for **1** (10 μM in DMF) during stepwise addition of $\mathbf{C_{60}}$ (up to 0.62 eqs, added as $10^{-3}$ M solution in *o*-DCB).

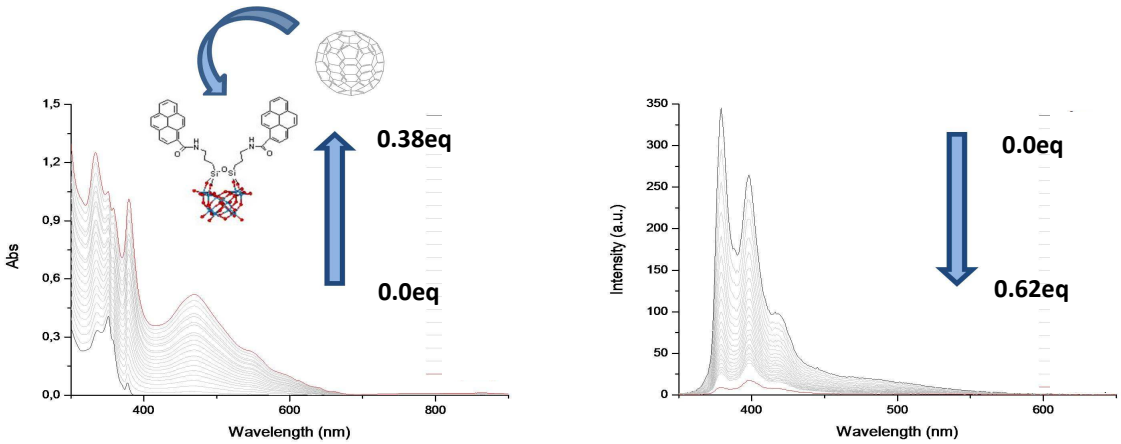


**Figure S10**. UV-vis (left) and Fluorescence (right, $\lambda_{ex}$ = 338 nm) spectra obtained for **1** (10 μM in DMF) during stepwise addition of $\mathbf{C_{70}}$ (up to 0.62 eqs, added as $10^{-3}$ M solution in *o*-DCB).

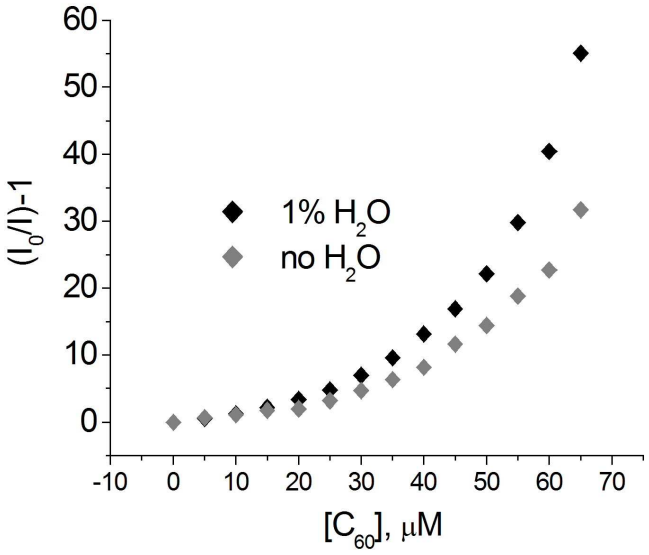


**Figure S11**. Stern-Volmer plot of fluorescence quenching of **1** [10 μM in DMF (grey diamonds) and DMF + 1% $H_2O$ (black diamonds)] by $C_{60}$ (0-7 eqs, added as $5x10^{-3}$ M solution in *o*-DCB); $\lambda_{em}$ = 397 nm.

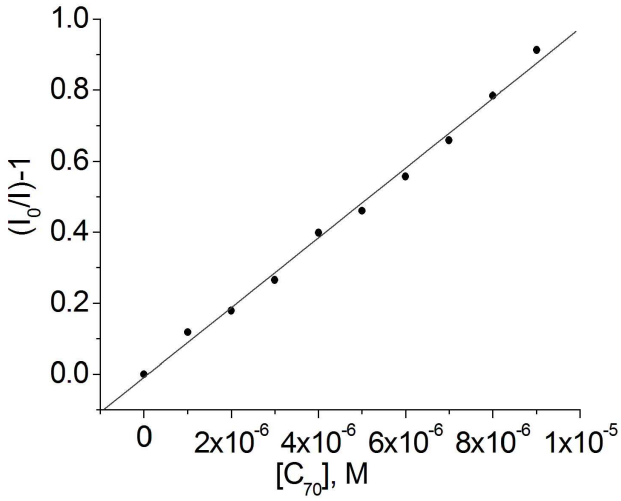


**Figure S12**. Stern-Volmer plot of the quenching of **1** fluorescence (10 μM) by $C_{70}$ (0-1 eqs, added as $10^{-3}$ M solution in *o*-DCB); $\lambda_{em}$ = 397 nm.

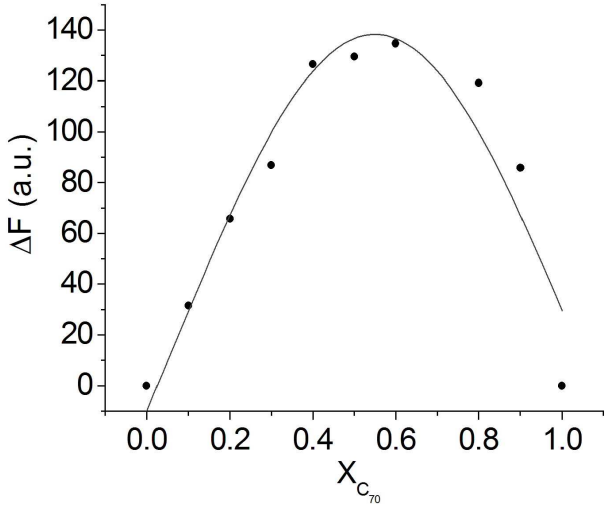


**Figure S13**. Job plot obtained for **1**@$C_{70}$ in DMF/*o*-DCB.

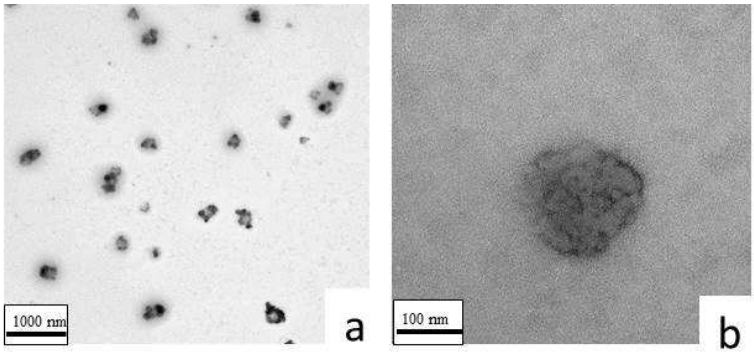


**Figure S14**. TEM images of **1**@$C_{60}$: (a) large area showing dispersed particles and (b) detailed image of a single aggregate.

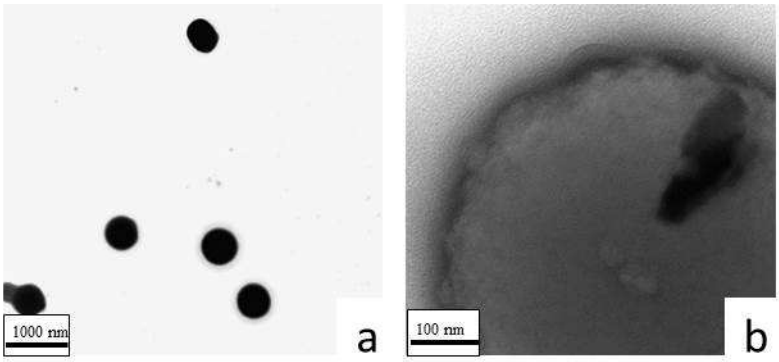


**Figure S15**. TEM images of **1**@$C_{70}$: (a) large area showing dispersed particles and (b) detailed image of a single aggregate.

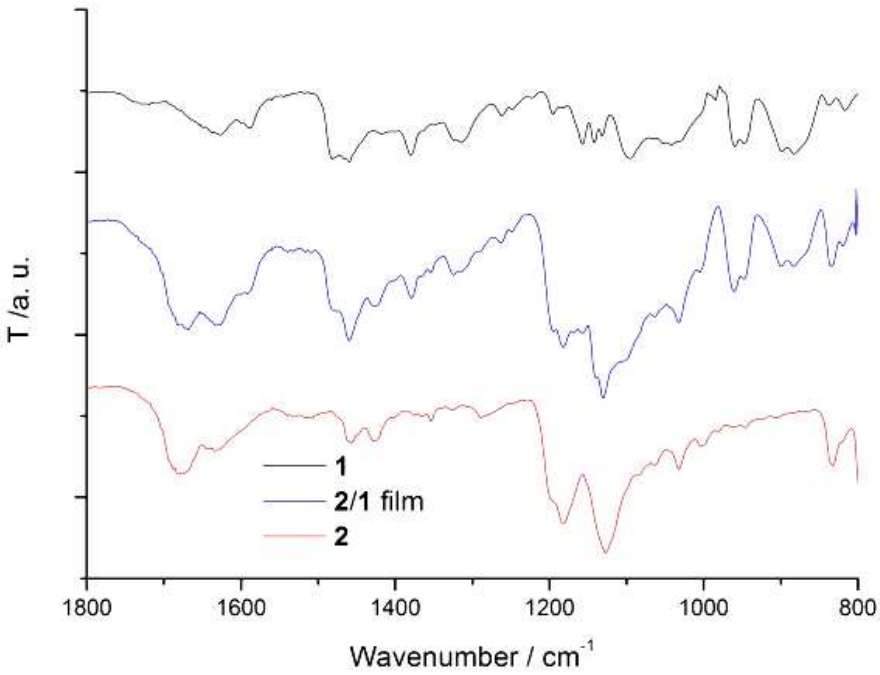


**Figure S16**. FT-IR spectrum in the range 1800-800 $cm^{-1}$ of cast film of **1** (black line) and L-S films of **2** and of the dyad **2**/**1** (blue line).

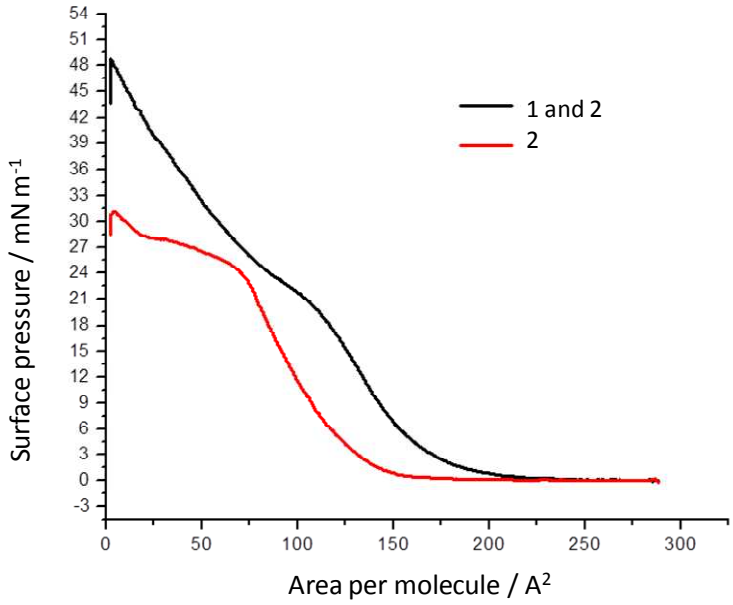


**Figure S17.** Langmuir curves of **2** on pure water subphase (red line) and with subphase containing **1** (dark line).

This journal is © The Royal Society of Chemistry 2014

**Table S1.** Brewster angle microscopy (BAM) images of the system **2**/**1** obtained at different surface pressure values

| **2** | **2 with 1 in subfase** |
|---|---|
| 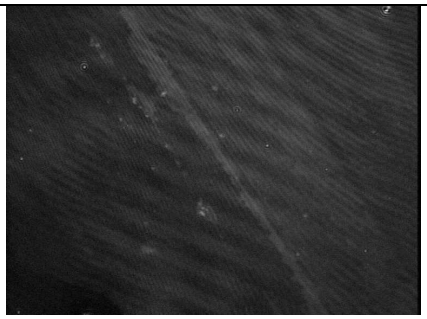 0.2 mN/m | 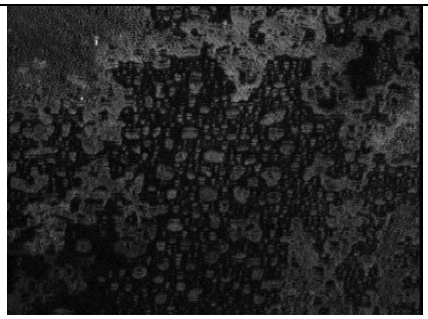 0.2 mN/m |
| 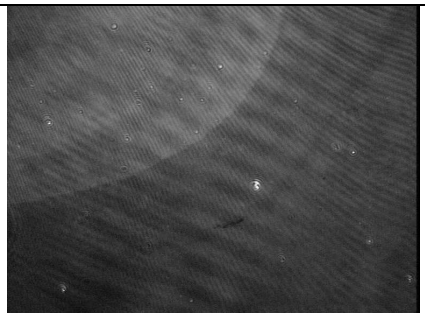 5.6 mN/m | 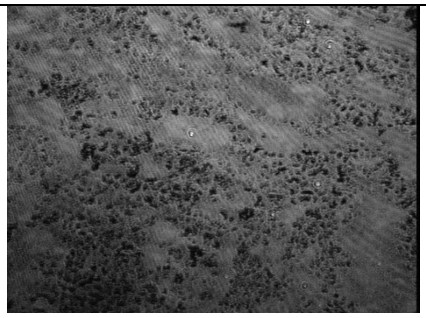 4.8 mN/m |
| 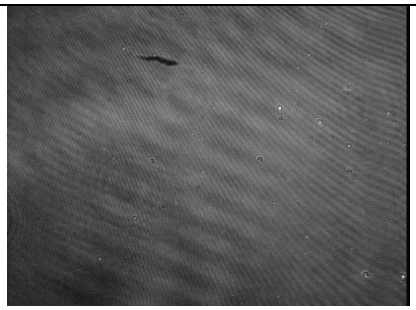 12 mN/m | 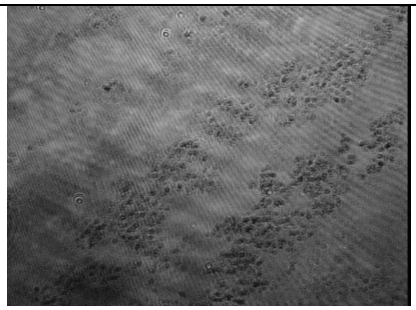 12 mN/m |
| 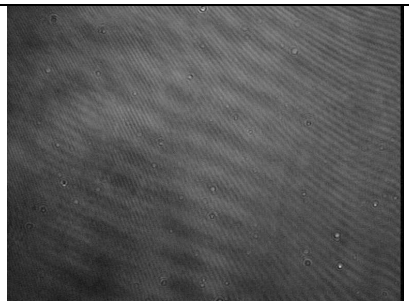 18 mN/m | 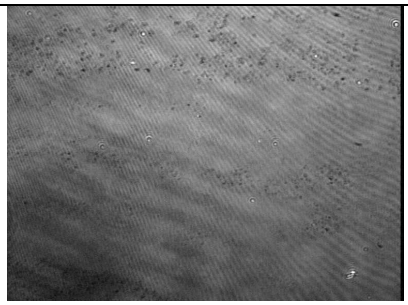 20 mN/m |
| 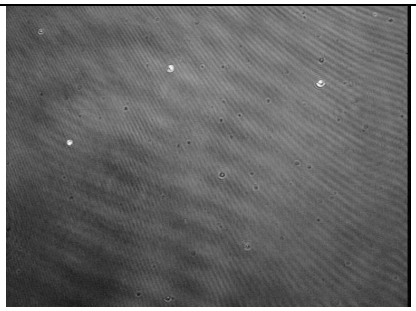 28 mN/m | 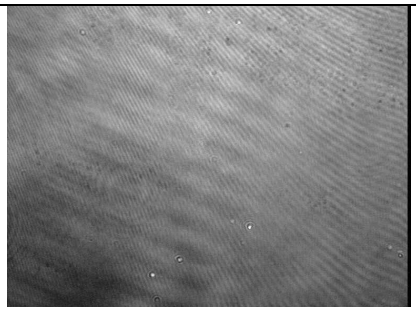 27.5 mN/m |

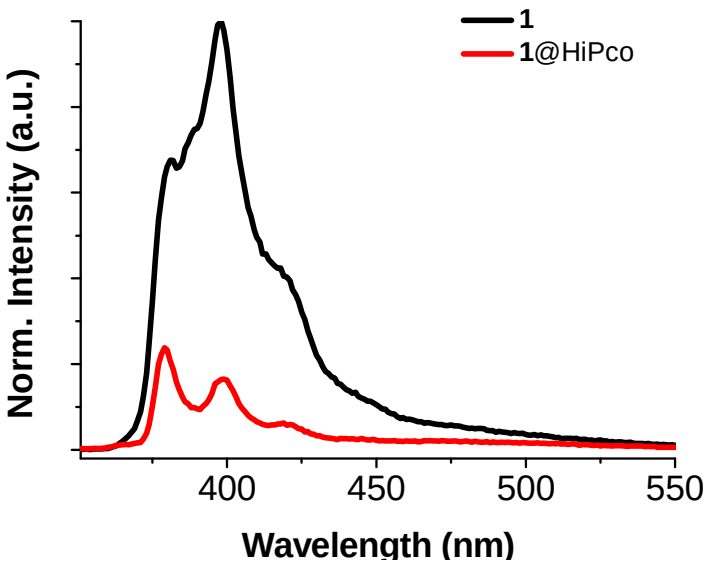


**Figure S18.** Emission spectra of **1**@HiPco in comparison with **1** in DMF.

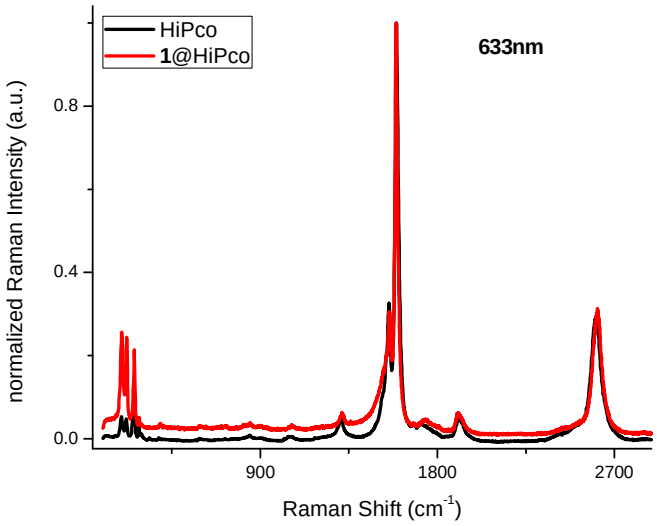


**Figure S19**. Raman spectra recorded at 633 nm of *p*-SWCNTs and (as-received HiPco) and **1**@HiPco normalized at the G band.

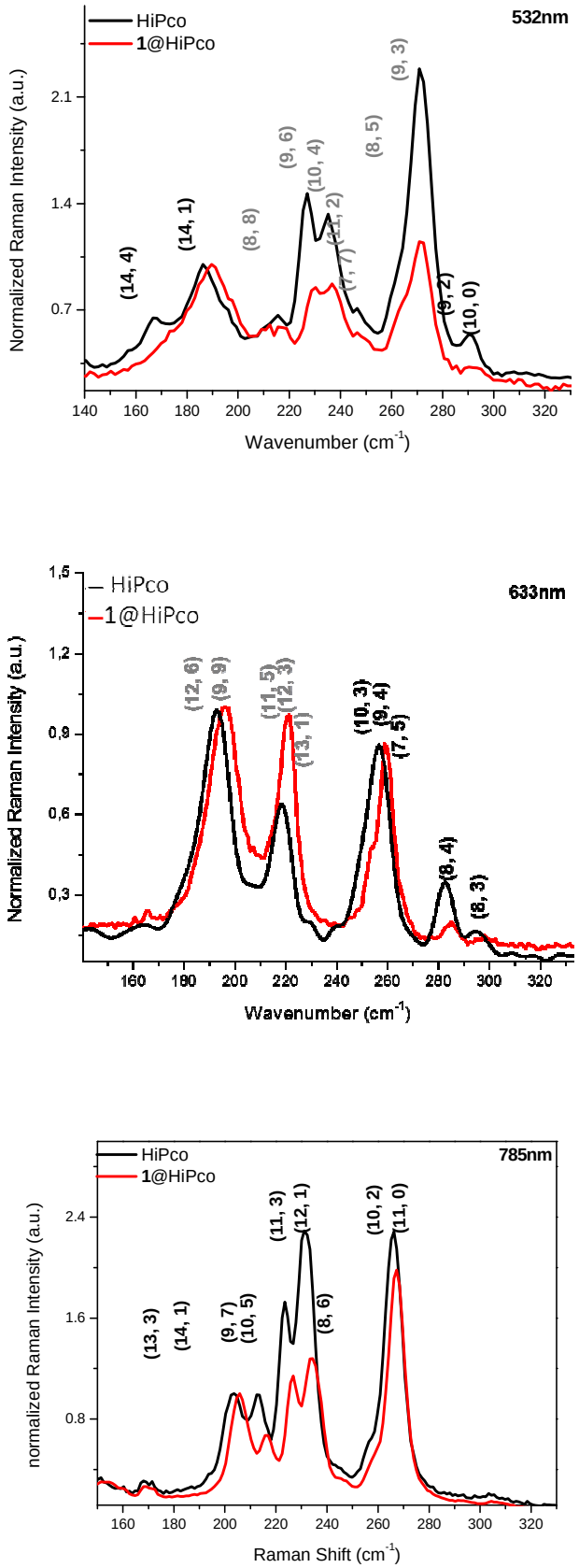


**Figure S20**. Normalized RBMs of p-SWCNT (as-received HiPco) and **1**@HiPco with related indices (metallic = black; semiconducting = grey) and diameters. Excitation wavelengths = 532 nm (top), 633 nm (middle, same as Fig.4b) and 785 nm (bottom).

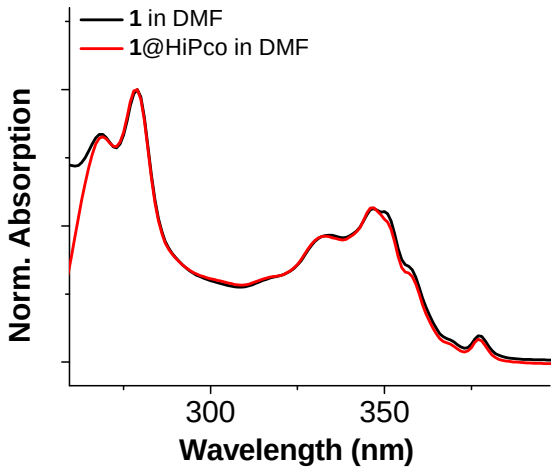


**Figure S21**. Normalized UV-Vis spectra of **1**@HiPco *versus* **1**; performed in DMF.

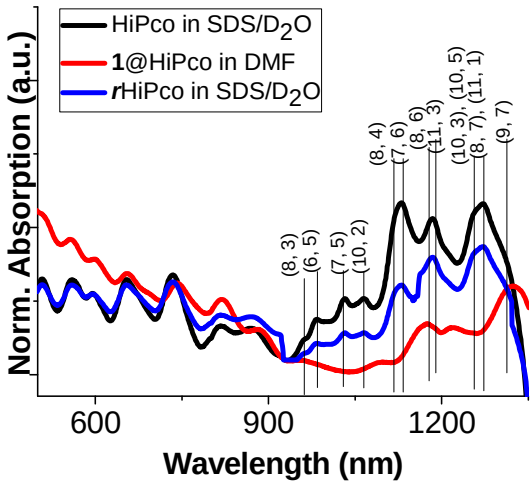


**Figure S22**. Normalized Vis-NIR spectra of **1**@HiPco in DMF *versus* pristine HiPco and the ***r***HiPco in SDS/$D_2O$. The identified chirality indices and diameters depicted are as follows: 962 nm (8,3), 984 nm (6,5), 1033 nm (7,5), 1063 nm (10,2), 1111 nm (8,4), 1120 nm (7,6), 1180 nm (8,6), 1203 nm (11,3), 1254 nm (10,3)/(10,5), 1265 nm (8,7)/(11,1), 1325 nm (9,7) and 1379 nm (10,6)/(12,2). All UV-Vis-nIR spectra are normalized to the absorbance minimum between the $S_{22}$ and $S_{11}$, at 938 nm for a better comparison.

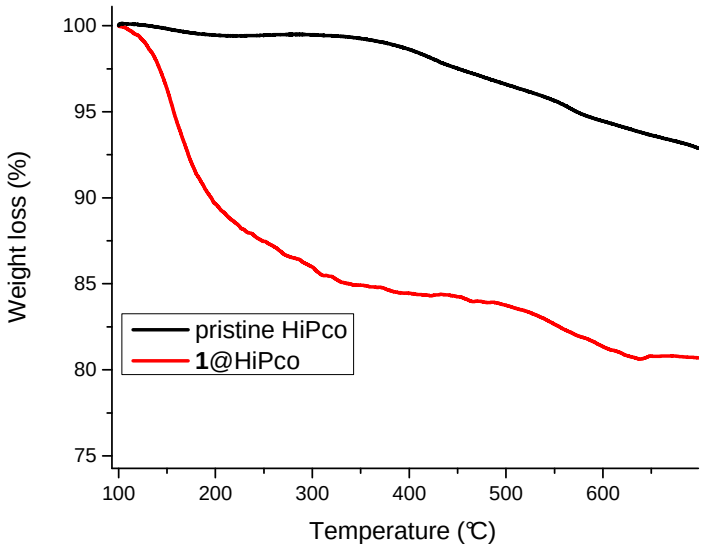


**Figure S23**. TGA of **1**@HiPco in comparison with the TGA of the pristine HiPco.

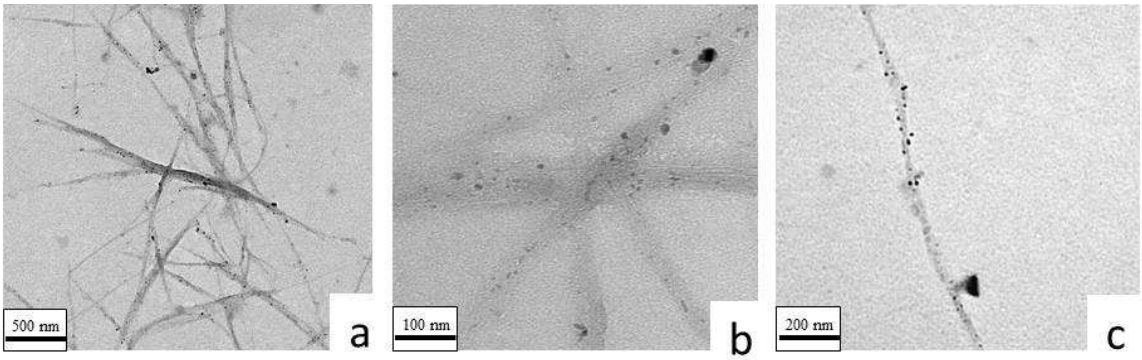


**Figure S24**. TEM images of **1**@HiPco: (a) large area of bundles; (b) enlargement of the previous image; and (c) smaller area with a small bundle of SWCNTs.

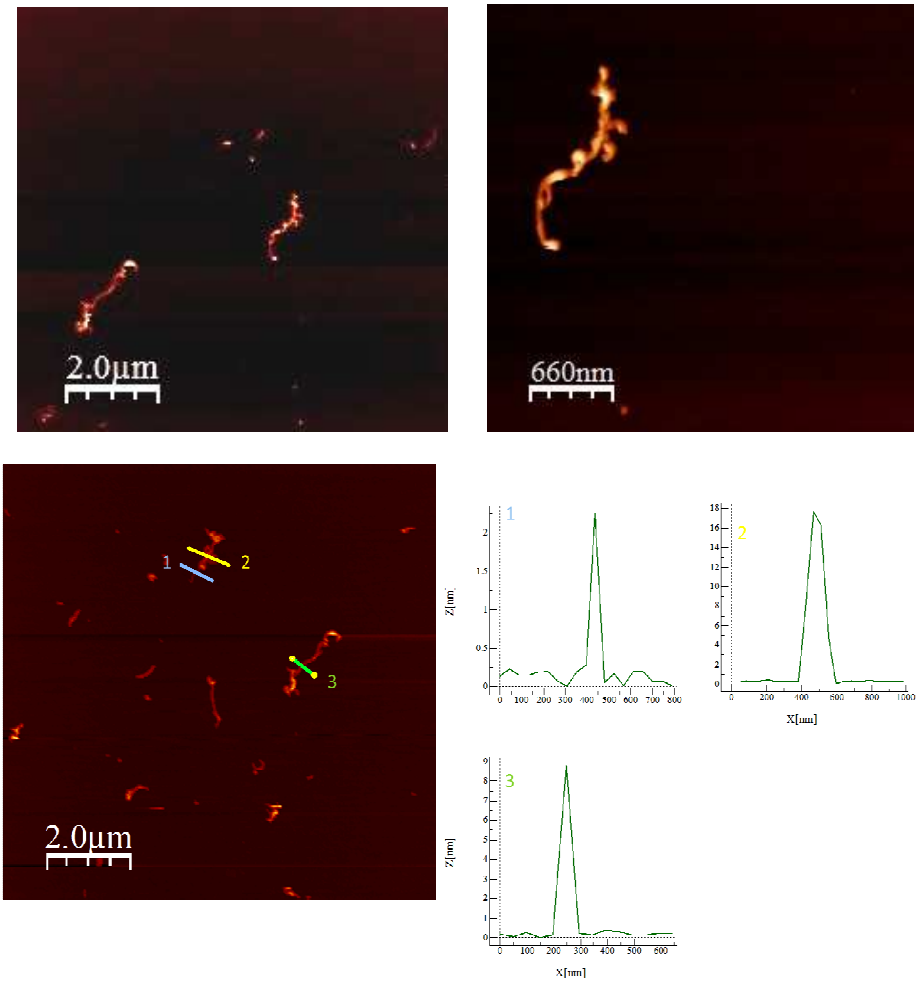


**Figure S25**. Top: AFM images of **1**@HiPco at different magnifications. Bottom: AFM of **1**@HiPco at a different substrate area, with the height profiles.

---

[i] M. Carraro, G. Modugno, G. Fiorani, C. Maccato, A. Sartorel and M. Bonchio, *Eur. J. Org. Chem.*, **2012**, 281.

[ii] J. Canny, A. Tézé, R. Thouvenot, G. Hervé, *Inorg. Chem.* 1986, **25**, 2114.

[iii] M. Carraro, L. Sandei, A. Sartorel, G. Scorrano and M. Bonchio, *Org. Lett.* 2006, **8**, 3671.